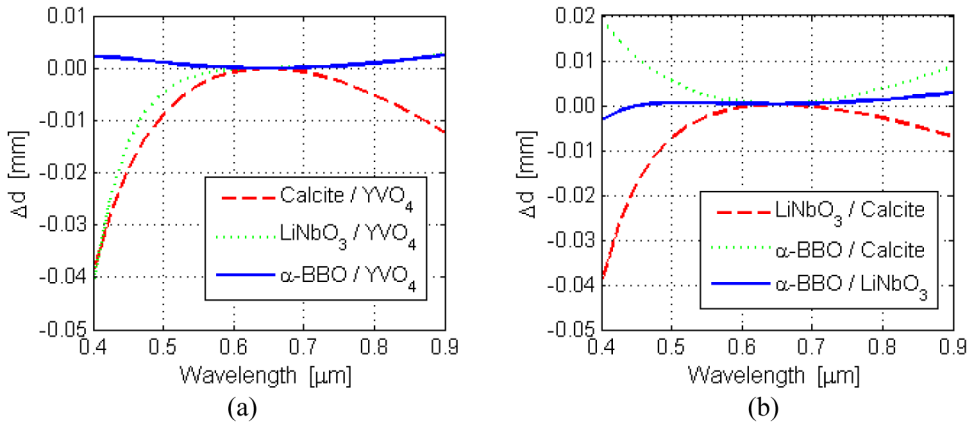

Fig. 4. The spectral variation of the lateral displacement relative to the nominal value for the ASPs that are made of pairing birefringent materials of (a) opposite sign and (b) same sign.

Table 2. Thickness ratio ρ, Individual Thickness t, Individual Lateral Displacement d, and Maximum CVLD $\mathrm{Max}|\Delta d|$ for the Nominal Lateral Displacement of 1 mm of the ASPs that are Made From Four Birefringent Crystals: YVO_4, Calcite, α-BBO, and $LiNbO_3$.

Pairing Materials	ρ	t_1 / t_2 (mm)	d_1 / d_2 (mm)	$\mathrm{Max}\|\Delta d\|$ (mm)
Calcite/YVO_4	1.506	18.51/12.29	2.8254/–1.8254	0.0394
$LiNbO_3$/YVO_4	2.000	45.72/22.6	2.3956/–3.3956	0.0415
α-BBO/YVO_4	4.070	14.39/3.54	1.5251/–0.5251	0.0025
α-BBO/$LiNbO_3$	2.035	12.47/6.13	1.3213/0.3213	0.0033
α-BBO/Calcite	2.702	20.21/7.48	2.1423/1.1423	0.0193
$LiNbO_3$/Calcite	1.328	15.99/12.04	0.8377/1.8377	0.0400

4. Ray tracing analysis

As a theoretical demonstration, the above-mentioned parameters of SPs and ASPs are inserted into Zemax software [28] with a 5 mm diameter pupil. Since the dispersion equations of some birefringent materials cited by Zemax software is not consist with Eqs. (10), the modifications of ZEMAX's glass catalogs must be done firstly to match up well with the theoretical calculation.

As discussed above, YVO_4 and α-BBO are two materials that are suitable for the designs of simple SP. After inserting the parameters that strictly copied from Table 1, the on-axis ray tracing configurations of the two simple SPs that made from YVO_4 and α-BBO are shown in Figs. 5(a) and 5(b) respectively. Correspondingly, the on-axis ray shearing diagrams at the last surface of the SPs are shown in Figs. 6(a) and 6(b) respectively. As can be seen, the lateral displacements reduce with the increases of wavelength, that is there are considerable CVLDs in the two simple SPs, although the CVLD of α-BBO is less than that of YVO_4. These phenomena consist with the above theoretical analysis.

#202883 - $15.00 USD Received 10 Dec 2013; revised 27 Jan 2014; accepted 15 Feb 2014; published 25 Feb 2014

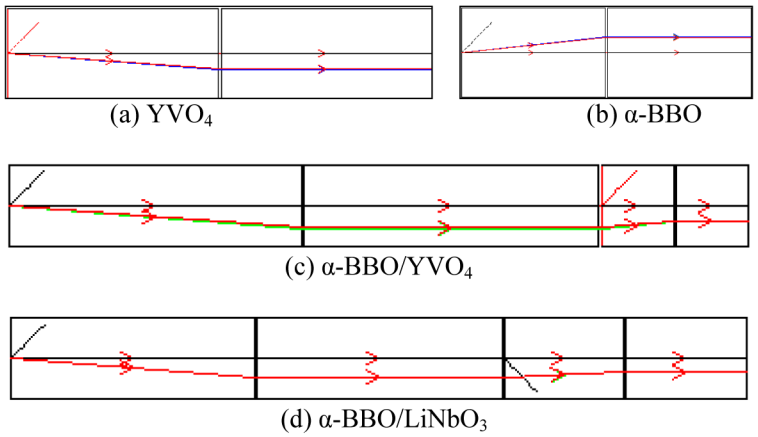

Fig. 5. The on-axis ray tracing configurations of two simple SPs and two ASPs with Zemax software (light passing from left to right).

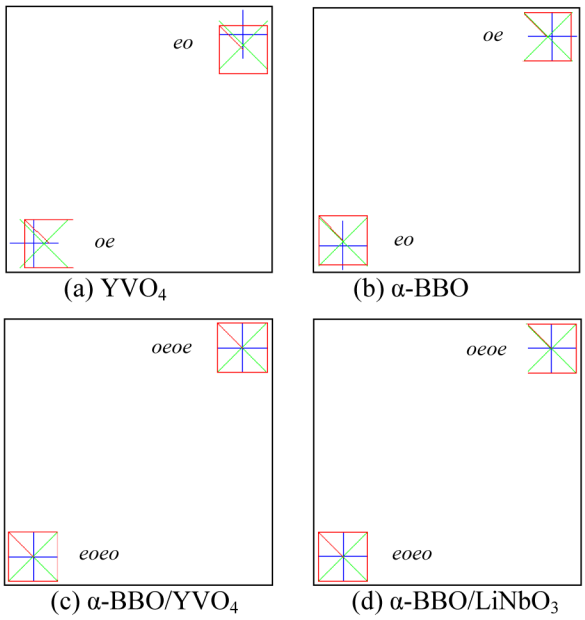

Fig. 6. The on-axis ray shearing diagrams at the last surface of two simple SPs and two ASPs. For visual purposes, one incident ray is shown. The symbols of red rectangle, green reticle and blue cross are used to illustrate the dispersion of different wavelengths.

Similarly, α-BBO/YVO_4 and α-BBO/$LiNbO_3$ are two pairing materials that are suitable for the designs of ASP. After inserting the parameters that strictly copied from Tab. 2, the on-axis ray tracing configurations of two ASPs that made from them are shown in Figs. 5(c) and 5(d) respectively. Figures 6(c) and 6(d) show the corresponding on-axis ray shearing diagrams at the last surface of the ASPs respectively. The CVLDs in the two ASPs almost reduce to zero and the emergent rays of different wavelengths overlap each other, although the thicknesses of the ASPs are considerably larger than that of the simple SPs. As can be seen, the ray tracing software simulation confirmed the developed theoretical model.

However, as described in section 2.1, the determination of the achromatic condition in Eq. (6a) is based on the neglect of the sin$i$ terms in Eqs. (1) and (3). For practical system, especially imaging system, the sin$i$ terms and higher order terms are inevitable. Figure 7

#202883 - $15.00 USD Received 10 Dec 2013; revised 27 Jan 2014; accepted 15 Feb 2014; published 25 Feb 2014

shows the off-axis ray shearing diagrams for the angle of incidence of 10°. As can be seen, the lateral displacements for different wavelengths still approach constant one, there are almost no residual CVLDs. That is the achromatization is also valid for non-normal incidence at paraxial angle. However, the emergent rays of different wavelengths do not overlap each other, and the shorter-wavelength rays shift away from the central-wavelength ray obviously. This issue has no any influence on the fringe pattern formed by the interferometric system that based on the ASPs, such as Fourier transform imaging spectrometry [2,4,5] and spectropolarimetry [11–13] and interferometry [14–16]. However, the issue should be treated carefully in the dual-beam imaging polarimeter [7], because the off-axis object point in the obtained polarization images for different wavelengths will not overlap each other. A band-pass or cut-off filter can be employed to deal with this problem.

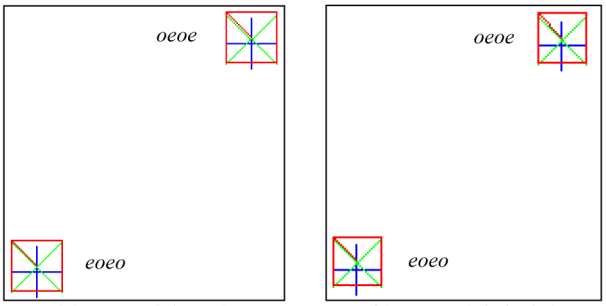

(a) α-BBO/YVO_4 (b) α-BBO/$LiNbO_3$

Fig. 7. The off-axis ray shearing diagrams at the last surface of ASPs. For visual purposes, one incident ray is shown. The symbols of red rectangle, green reticle and blue cross are used to illustrate the dispersion of different wavelengths.

5. Summary

In conclusion, this paper describes the achromatization principle of SP and proposes an effective procedure for the design of ASP. The ASP can be achieved by combining two SPs that are made of two materials with opposite sign or same sign of birefringence. The material selection depends on the advantages of birefringence, achromatization, size, cost, and availability. The theoretical simulation and ray tracing results show that two pairing materials, α-BBO/YVO_4 and α-BBO/$LiNbO_3$, are suitable to the achievement of achromatization among four suggested birefringent materials: YVO_4, Calcite, α-BBO and $LiNbO_3$. The reduction in the chromatic variation of lateral displacement can be reduced by an order of magnitude across the specified spectral range 0.4 μm to 0.9 μm. The thicknesses of the two SPs are determined by the nominal center wavelength of 0.65 μm. The principle of achromatization has potential benefits at all wavelengths where SP may be used, and the price to pay is the increase of size.

Acknowledgments

The authors thank the anonymous reviewers for their helpful comments and constructive suggestions. The work was supported by the Scientific Research Support Program for New Teacher of Xi'an Jiaotong University of China, the Fundamental Research Funds for the Central Universities of China (xjj2013044), the Specialized Research Fund for the Doctoral Program of Higher Education of China (20130201120047), the National Natural Science Foundation of China (61275184), and the National High Technology Research and Development Program of China (2012AA120211).